Time dependence of donor–acceptor electron transfer and back transfer in solid solution

Y. Lin, R. C. Dorfman, and M. D. Fayer
Department of Chemistry, Stanford University, Stanford, California 94305

(Received 18 July 1988; accepted 21 September 1988)

Electron transfer from an optically excited donor to randomly distributed acceptors followed by electron back transfer is treated theoretically for donors and acceptors in a rigid solution. The forward electron transfer process is described in terms of the excited state population probability $P_{ex}(t)$ of the donor molecules, while the electron back transfer from the radical anion to the radical cation is characterized by $P_{ct}(t)$, the donor cation state population probability. Exact expressions for the ensemble averages $\langle P_{ex}(t)\rangle$ and $\langle P_{ct}(t)\rangle$ are derived. Numerical calulations are presented for the cation probabilities, the average cation–anion separation distance $\langle R(t)\rangle$, and the average cation existence time $\langle \tau(R)\rangle$, using parameters which characterize the forward and back transfer distance dependent rates. Relationships among $\langle P_{ex}(t)\rangle$, $\langle P_{ct}(t)\rangle$ and the intermolecular interaction parameters provide detailed insights into the distance and time dependence of the flow of electron probability in an ensemble of donors and acceptors. The theoretical expressions can be used to calculate experimental observables. In particular, picosecond transient grating experiments are analyzed, and it is shown that by combining grating experiments (or other ground state recovery experiments) with fluorescence experiments it is possible to obtain the intermolecular interaction parameters for both forward and back transfer and a detailed description of the dynamics. The calculations presented here for rigid solutions are the precursor to the inclusion of diffusive motion of donors and acceptors to describe the dynamics of coupled electron transfer and back transfer in liquid solutions.

I. INTRODUCTION

In a system in which there are donors (low concentration) and acceptors (high concentration) randomly distributed in a solid solution, optical excitation of a donor can be followed by transfer of an electron to an acceptor.[1] Once electron transfer has occurred, there exists a ground state radical cation (D^+) near a ground state radical anion (A^-), Since the thermodynamically stable state is the neutral ground state D and A, back transfer will occur. In liquid solution, back transfer competes with separation by diffusion. Separated ions are extremely reactive and can go on to do useful chemistry.[2]

There has been considerable interest in the process of electron transfer with eventual recombination. A number of investigations of photosynthetic electron transfer pathways, both time resolved and steady state, have been reported.[1–4] In photosynthesis, the complex structure of the system of a donor and a sequence of acceptors inhibits back transfer, and efficient charge separation takes place. There have also been studies of transfer and recombination in liquid solutions.[5–10] Because of the complexity of the problem of coupled forward and back transfer in a system undergoing molecular diffusion, a detailed statistical mechanical theory describing the dynamics is lacking. Here the focus is on a system of donors and acceptors which are in fixed positions. This permits the ensemble averaged dynamics of the coupled forward and back transfer processes to be isolated from the influence of molecular diffusion. In a subsequent publication, we will present an extension of this work to include diffusion in liquid solutions.[11]

A great deal of effort has been devoted to modeling the microscopic electron transfer rate.[1,2,12–15] It has been shown[16–19] that a transfer rate which is exponentially dependent on distance works well for electron transfer over a considerable range of distances. We employ this form of the microscopic electron transfer rate to describe both the forward and back electron transfer for a particular donor–acceptor pair.

The forward transfer process is relatively straightforward to model.[16,17,19–21] The forward transfer process involves the interaction of a donor with acceptors which are randomly distributed in space. For a donor–acceptor electron transfer rate which falls off exponentially with distance, Inokuti and Hirayama[20] have developed a statistical mechanics theory describing the time dependence of the ensemble averaged forward transfer.

The back transfer problem is more complex. The distribution of distances between the ions D^+ and A^- is not random. It is determined by the details of the forward transfer process. The distribution will be strongly biased toward small separations. After electron transfer the system consists of a cation near an anion. Transfer from the anion to a neutral acceptor is not included since there is no net driving force for the transfer and barriers for electron tunneling are generally large.[2] Transfer from the anion to a cation which was not the original source of the electron is not included because the concentration of donors is assumed to be low and the concentration of donor cations is even lower. The statistical mechanical theory presented below is an exact solution to the model problem outlined above. The theory calculates the time dependent probabilities that the donor is an

 0021-9606/89/010159-12$02.10

excited singlet, is a cation, or is a neutral in its ground electronic state. From these results the average ion-pair separation as a function of time and the average time for ion-pair existence as a function of distance are calculated. The effect a particular acceptor has on the ion-pair probability, with the influence of the other acceptors properly accounted for, as a function of time and distance are also calculated. The results provide an excellent picture of the dynamics of an ensemble of electron transfer systems.

The theory presented here, when used with a ground state time dependent recovery experiment, gives the parameters characterizing the back transfer distance dependent dynamics. The results obtained from experiment will give the microscopic electron transfer rate. The observables (state probabilities), not the rates, are properly averaged over the nonrandom distribution of distances. The theory is used to calculate the experimental observable in a picosecond transient grating experiment. A brief account of experimental results has been presented,[22] and a detailed account will be given elsewhere.[23] For a particular molecular system, the use of this theory in conjunction with experiment provides a comprehensive description of electron transfer and recombination dynamics.

II. THEORETICAL DEVELOPMENT

In this section we derive the donor excited state population function $P_{ex}(t)$, and the donor cation state population function $P_{ct}(t)$. The exact expression for the ensemble averaged $\langle P_{ex}(t)\rangle$ and $\langle P_{ct}(t)\rangle$ are given. In the model, low concentration donors and high concentration acceptors are randomly distributed and held fixed in a rigid matrix. It is assumed that the donor has only one accessible electronic excited state, and the acceptor has only one acceptor state. All states are singlets. The concentration of donor molecules is low enough that donor–donor electronic excitation transfer does not occur. Because the thermodynamic lowest energy state of the system is a neutral donor and a neutral acceptor and spatial diffusion of the molecules does not occur in the solid solution, back transfer is geminate. Thus, following electron transfer from the excited neutral donor to an acceptor, the anionic acceptor will not transfer the electron to a neutral acceptor, but only back to the cationic donor. The fast time dependent structural relaxation upon ion formation is not included in the model, although it could influence the time dependence at very short times. The transfer rates[16–19] are exponentially decaying functions of distance.

At time $t = 0$ an ensemble of dilute donors is optically excited. In the absence of acceptors, the probability of finding the donor still excited at time t, $P_{ex}(t)$, decays exponentially with the excited state lifetime τ, i.e., $P_{ex}(t) = \exp(-t/\tau)$. When acceptors are present the probability decreases more rapidly due to the addition of the electron transfer pathway for quenching the electronic excited state. Electron transfer creates a ground state radical cation (D^+) near a ground state radical anion (A^-). Since the thermodynamically stable state consists of the neutral ground state of D and A, electron back transfer will occur. A diagrammatic representation of these processes is shown in Fig. 1.

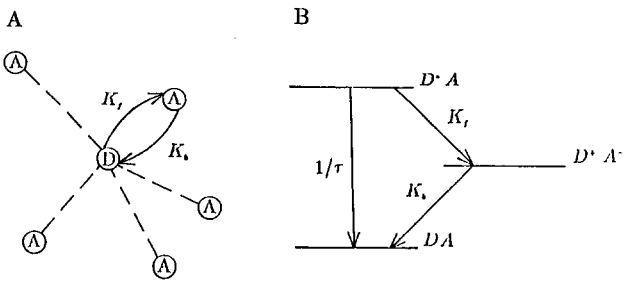

FIG. 1. (A) A diagrammatic representation of electron transfer with recombination. The solid lines represent actual transfer events. The dashed lines show other possible paths. (B) Energy level diagram. The diagram shows only one of the n acceptors.

The three processes, excited state decay, forward electron transfer, and electron back transfer have the following rate constants:

$$k = 1/\tau \quad \text{excited state decay,} \tag{1a}$$

$$K_f = \frac{1}{\tau}\exp\left(\frac{R_0 - R}{a_f}\right) \quad \text{forward transfer,} \tag{1b}$$

$$K_b = \frac{1}{\tau}\exp\left(\frac{R_b - R}{a_b}\right) \quad \text{back transfer,} \tag{1c}$$

where R is the donor–acceptor separation. R_0 and R_b are used to parametrize the distance scales of forward and back transfer.[17,19,20] a_f and a_b characterize the fall off of the electronic wave function overlap of the neutral donor and acceptor states, and the ionic states, respectively.[17,19,20] τ is the donor fluorescence lifetime.

The differential equations describing the processes for a donor and n acceptors having a fixed configuration of donor–acceptor separations given by the set of distances R_i in a volume V are:

$$\frac{dP_{ex}(t)}{dt} = -\left[k + \sum_{i=1}^{n} K_f(R_i)\right]P_{ex}(t), \tag{2}$$

$$\frac{dP^i_{ct}(t)}{dt} = K_f(R_i)P_{ex}(t) - K_b(R_i)P^i_{ct}(t), \quad i = 1,\ldots,n, \tag{3}$$

where each R_i is the distance from the donor to the ith acceptor. $P_{ex}(t)$ is the probability of finding the donor in its excited state. $P^i_{ct}(t)$ is the probability of finding the donor in its cation state with the ith acceptor in its anion state. The $\Sigma_{i=1}^{n} P^i_{ct}(t)$ describes the total probability of finding the donor in its cation state. The terms multiplying $P_{ex}(t)$ in Eq. (2) accounts for processes which remove the donor molecule from its excited state. In Eq. (3) the factor $K_f(R_i)P_{ex}(t)$ describes electron transfer which takes the donor to its cationic state. Similarly the term $-K_b(R_i)P^i_{ct}(t)$ accounts for electron back transfer from the ith acceptor (anion) to the donor (cation), returning the donor cation to its neutral ground state.

In the forward transfer process, donor molecules can transfer an electron to any acceptor with the transfer rate determined by the D–A separation. Back transfer is distinctly different. The anion can back transfer the electron only to

the original donor molecule (now a cation). For an ensemble of initially excited donors, the distribution of anion–cation separations produced by forward electron transfer is not random but is dependent on the details of the forward transfer. The ensemble average of Eq. (3) properly accounts for this time dependent distribution.

The solution of Eq. (2) is straightforward:

$$P_{ex}(t) = e^{-kt} \exp\left[-\sum_{i=1}^{n} K_f(R_i)t \right]. \tag{4}$$

The decay described by $P_{ex}(t)$ depends on the particular acceptor configuration considered. Of significance is the ensemble average $\langle P_{ex}(t) \rangle$ over all possible configurations. Up to moderate concentration $\langle P_{ex}(t) \rangle$ is given by Inokuti and Hirayama (IH). The IH theory does not include excluded volume effects. In the Appendix, the theory presented below will be reanalyzed taking into account excluded volume, and excluded volume effects are discussed in Sec. III D. Here the molecules are considered to be point particles, and excluded volume does not come into play. The analysis of the Appendix shows that this is a reasonable approximation up to moderate concentration. The IH result is

$$\langle P_{ex}(t) \rangle = e^{-t/\tau} \exp[-(C/C_0)\gamma^{-3} g(e^{\gamma} t/\tau)], \tag{5}$$

where C is the acceptor concentration and C_0 is given by $C_0 = 3/(4\pi R_0^3)$, γ is R_0/a_f with

$$g(Z) = 3\int_0^{\infty} [1 - \exp(-Ze^{-y})] y^2 \, dy. \tag{6}$$

Instead of directly solving Eq. (3) for $P_{ct}^i(t)$, then performing the ensemble average of $P_{ct}^i(t)$ and passing to the thermodynamic limit, we first perform the ensemble average over all possible spatial configurations of $n-1$ acceptors in a volume V for each term of Eq. (3):

$$\left\langle \frac{dP_{ct}^i(t)}{dt} \right\rangle_{n-1} = \langle K_f(R_i) P_{ex}(t) \rangle_{n-1} - \langle K_b(R_i) P_{ct}^i(t) \rangle_{n-1}, \tag{7}$$

where $\langle \ \rangle_{n-1}$ denotes an average over all spatial coordinates except the ith spatial coordinate. $\langle P_{ct}^i(t) \rangle_{n-1}$ is the averaged probability of finding the donor in its cation state with an acceptor at R_i in its anion state. Since the spatial distribution of acceptors at different points is uncorrelated and the ensemble averaging procedure is independent of the time derivative, Eq. (7) can be rewritten as

$$\frac{d}{dt}\langle P_{ct}^i(R_i,t) \rangle_{n-1} = K_f(R_i)\langle P_{ex}(t) \rangle_{n-1} - K_b(R_i)\langle P_{ct}^i(R_i,t) \rangle_{n-1}. \tag{8}$$

Casting the problem in the form of Eq. (8) has an important advantage. It reduces the many particle problem in Eq. (3) to a two particle problem. This is the key step which makes the solution of this problem tractable.

The solution of the differential equation (8) is now straightforward:

$$\langle P_{ct}^i(R_i,t) \rangle_{n-1} = \int_0^t K_f(R_i) e^{-K_b(R_i)(t-t')} \langle P_{ex}(t') \rangle_{n-1} \, dt'. \tag{9}$$

Equation (9) is an exact expression for the probability of a donor molecule being a cation with an anion at position R_i. $K_f(R_i)\langle P_{ex}(t') \rangle_{n-1}$ [under the integration sign in Eq. (9)] is the rate of an excited donor transferring an electron at time $= t'$, i.e., the cation creation probability, and the exponential term $\exp(-K_b(R_i)(t-t'))$ reflects the probability that a cation was created at time $= t'$ and still survives at a later time t. Hence the total probability of finding a cation at time t with the anion at R_i is the product of the cation creation probability and cation survival probability, integrated over all the times from zero to t. Equation (9) was obtained for the initial condition that at $t = 0$ all the molecules are neutral, i.e., $\langle P_{ct}^i(R_i,0) \rangle_{n-1} = 0$.

The explicit expression for $\langle P_{ex}(t) \rangle_{n-1}$ is obtained by averaging Eq. (4) over all acceptor coordinates except the ith acceptor coordinate. The result is

$$\langle P_{ex}(t) \rangle_{n-1} = e^{-t/\tau} e^{-K_f(R_i)t} [1 - \gamma^{-3}(R_0/R_v)^3 g(e^{\gamma} t/\tau)]^{n-1}, \tag{10}$$

where $R_v^3 = 3V/(4\pi)$, V is the volume in which the acceptors are distributed.

We can now substitute Eq. (10) into Eq. (9) which gives

$$\langle P_{ct}^i(R_i,t) \rangle_{n-1} = K_f(R_i) e^{-K_b(R_i)t} \times \int_0^t \exp\{ -[1/\tau + K_f(R_i) - K_b(R_i)]t' \} \times [1 - (R_0/R_v\gamma)^3 g(e^{\gamma} t'/\tau)]^{n-1} dt'. \tag{11}$$

The total time dependent probability of a donor molecule being a cation is found by averaging over all possible spatial positions of R_i, and summing over all i acceptors:

$$\langle P_{ct}(t) \rangle = \sum_{i=1}^{n} \frac{4\pi}{V} \int_0^{R_v} \langle P_{ct}^i(R_i,t) \rangle_{n-1} R_i^2 \, dR_i. \tag{12}$$

Each term in the sum is identical thus

$$\langle P_{ct}(t) \rangle = \frac{4\pi n}{V} \int_0^{R_v} \langle P_{ct}^i(R_i,t) \rangle_{n-1} R_i^2 \, dR_i. \tag{13}$$

At this point we pass to the thermodynamic limit, i.e., we take the limit as the number of acceptors n and the volume V go to infinity while keeping their ratio constant. In this limit, n/V becomes the concentration of acceptors C. The result gives the total probability that the donor is a cation:

$$\langle P_{ct}(t)\rangle = 4\pi C\int_0^\infty K_f(R_i)e^{-K_b(R_i)t}\int_0^t \exp\{-[K_f(R_i)-K_b(R_i)]t'\}\times e^{-t'/\tau}\exp\left[-\left(\frac{C}{\gamma^3 C_0}\right)g\left(e^{\gamma}\frac{t'}{\tau}\right)\right]dt'\,R_i^2\,dR_i$$

$$= 4\pi C\int_0^\infty K_f(R_i)e^{-K_b(R_i)t}\int_0^t \exp\{-[K_f(R_i)-K_b(R_i)]t'\}$$

$$\times e^{-t'/\tau}\exp\left(-4\pi C\int_0^\infty (1-e^{-t'K_f(R_j)})R_j^2\,dR_j\right)dt'\,R_i^2\,dR_i. \tag{14}$$

The last integral in Eq. (14) is the $g(Z)$ function [Eq. (6)] written explicitly with $y = R/a_f$.

Equation (14), which involves a double integral over space and time, can be readily evaluated numerically. The function inside the integral has an upper bound when $K_f(R)$ and $K_b(R)$ have the form given Eqs. (1b) and (1c). In the next section we shall discuss the physical properties of $\langle P_{ct}(t)\rangle$.

III. RESULTS AND DISCUSSION

In the previous section we obtained expressions for the time dependent probabilities that a donor is in its excited state or in its cationic state. Having the expressions for $\langle P_{ex}(t)\rangle$ and $\langle P_{ct}(t)\rangle$, the ensemble averaged probability that a donor is in its neutral ground state, $\langle P_g(t)\rangle$, is $\langle P_g(t)\rangle = 1 - \langle P_{ex}(t)\rangle - \langle P_{ct}(t)\rangle$. From these probability functions, it is possible to calculate a number of interesting time dependent properties that are characteristic of electron transfer and back transfer in an ensemble of donors and acceptors randomly distributed in a rigid solution. These are discussed in the following sections.

A. The many particle nature of the problem

The electron transfer rates in Eqs. (1b) and (1c) depend exponentially on distance. Therefore electron transfer is a relatively short range process. The distance scale is on the order of R_0 and R_b. The short range nature of the transfer rates has led some to believe that only the single nearest acceptor is important in determining the dynamics of electron transfer and recombination.[16] In this sense the problem would reduce to a one acceptor calculation. Using the results of Sec. II, it is possible to address the question of the many particle nature of this problem.

Prior to passing to the thermodynamic limit, the problem is cast in terms of a finite number of acceptors. Equation (14) gives the cation probability for an ensemble having an infinite number of acceptors and concentration, C. Equation (13) can be used to obtain the same quantity for any finite number of acceptors n in a volume V such that the ratio is C. Thus Eq. (13) gives the probability that the donor is a cation as a function of time and the number of acceptors.

In Fig. 2 we show the time dependent cation probability for 1, 2, 3, 4, 8, and an infinite number of acceptors. The parameters used in the calculation are given in the figure caption. In Fig. 2(A), the concentration is relatively low, i.e., $C = 0.05$ M. While the curves have the same general shape, even at low concentration the one acceptor calculation is significantly different from the infinite acceptor result. Although the two acceptor calculation is substantially better, the other curves show that convergence is quite slow. Figure 2(B) shows a calculation for a relatively high concentration, $C = 0.5$ M. Here the one acceptor result is very inaccurate, and again the convergence is slow. The results presented in Fig. 2 demonstrate the many particle nature of this problem. It is clearly insufficient to consider a single acceptor or a small number of acceptors.

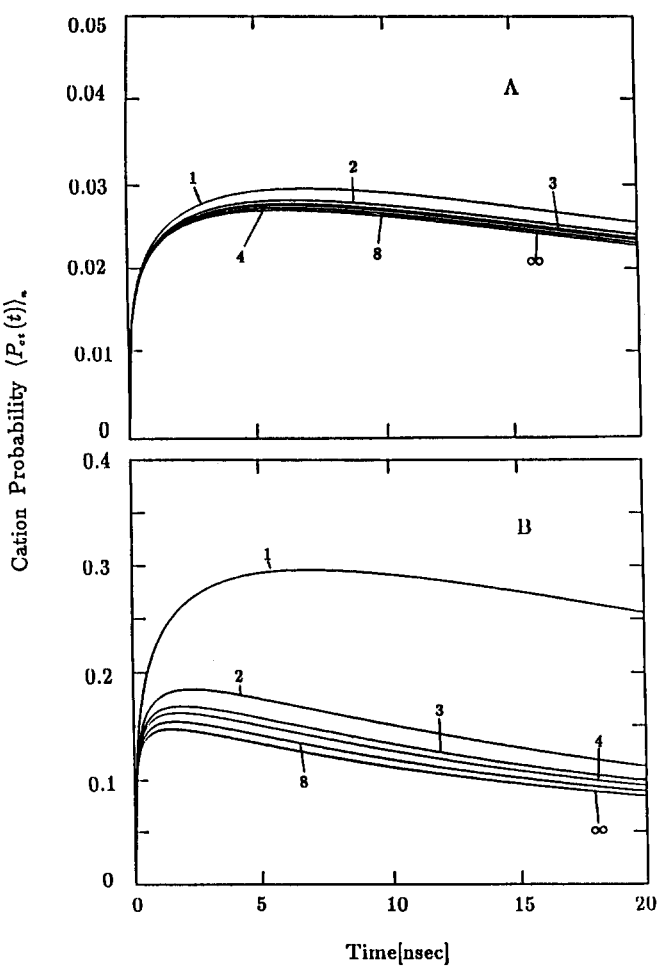

FIG. 2. 1, 2, 3, 4, 8, and infinite particle calculations for the probability that the donor is a cation. As the number of particles increases the result approaches the thermodynamic limit. The fact that the 8 particle result has not yet converged demonstates the need to consider this as a many particle problem. In (A) the concentration is $C = 0.05$ M, and (B) $C = 0.5$ M. The other parameters are $R_0 = R_b = 10$ Å, $a_f = a_b = 1$ Å, and $\tau = 16$ ns.

B. Cation probabilities

Calculations of the ensemble averaged time evolution of the cation probability $\langle P_{ct}(t)\rangle$ are presented in Fig. 3 for various electron transfer parameters R_0, R_b, a_f, and a_b. For these calculations, the concentration is 0.1 M, and the excited state lifetime is 16 ns. The other parameters are given in the figure caption for each curve. One observes that $\langle P_{ct}(t)\rangle$ rises rapidly within the first nanosecond, reaches its maximum value, and then slowly decays to zero. At $t=0$, the donor molecules are in the excited state, and no radical pairs exist. Hence $\langle P_{ct}(0)\rangle = 0$. After excitation, a fraction of the systems in the ensemble will fluoresce and a fraction will undergo forward electron transfer. As a result of electron transfer, the cation state population builds up. The onset of radical pair formation marks the beginning of the recombination process. The competition between the probabilities of forward electron transfer and recombination determines the detailed shape of $\langle P_{ct}(t)\rangle$. Curves A, B, and E in Fig. 3 demonstrate that the maximum cation probability increases as forward transfer parameter R_0 increases, and decreases as back transfer parameter R_b increases. Even for the relatively small changes in the R parameters the influence on the cation probability is dramatic. In going from curve B to curve C, it is seen that reducing both R_0 and R_b the same amount reduces the maximum cation probability and shifts the maximum to longer time. Comparison of curves B and D shows that reducing the magnitudes of a_f and a_b reduces the time to reach a maximum in ion pair probability but diminishes the maximum probability. In the next subsection it will be shown that short times correspond to short distance transfer events, while the long time behavior is dominated by the formation and recombination of ion pairs with large ion separations.

The time dependent cation probability can be looked at in several ways. For a system of randomly distributed donors and acceptors, it is possible to look at the influence of a particular acceptor on the cation probability as a function of time and the donor–acceptor separation. To investigate the effect of the ith acceptor, it is necessary to average over the positions of all other acceptors, since they in part determine the rate of electron transfer to the ith acceptor when it is at location R_i. The expression for this conditional probability $\langle P^i_{ct}(R_i,t)\rangle$ is given by Eq. (11). In the thermodynamic limit the expression is

$$\langle P^i_{ct}(R_i,t)\rangle = K_f(R_i)e^{-K_b(R_i)t} \times \int_0^t \exp\{-[K_f(R_i)-K_b(R_i)]t'\} \times \exp\left[-\frac{t'}{\tau}-\left(\frac{C}{\gamma^3 C_0}\right)g\left(e^{\gamma}\frac{t'}{\tau}\right)\right]dt'. \tag{15}$$

It is informative to plot cross sections of this two-dimensional surface as functions of time at constant distance and distance at constant time. These plots are shown in Figs. 4 and 5.

$\langle P^i_{ct}(R_i,t)\rangle$ vs distance for a unit volume element about R_i is displayed in Fig. 4 for the time t varying from 0.01 to 100 ns. The electron transfer parameters are $a_f = 1.0$ Å, $a_b = 1.0$ Å, $R_0 = 10.0$ Å, and $R_b = 10.0$ Å, and the concentration of acceptors is 0.1 M. The excited state lifetime is 16 ns. These are the same parameters used to calculate curve C in Fig. 3. For a given time, the curves show the probability of having ion pairs with various ion separation distances. Consider one of the curves for a particular time t. If each point on the curve is multiplied by $4\pi C R_i^2$ and the curve is integrated, the resulting value corresponds to the value of curve C in Fig. 3 at the time t.

In Fig. 4, for each time, there is a most probable cation–anion separation, and this distance increases as t increases.

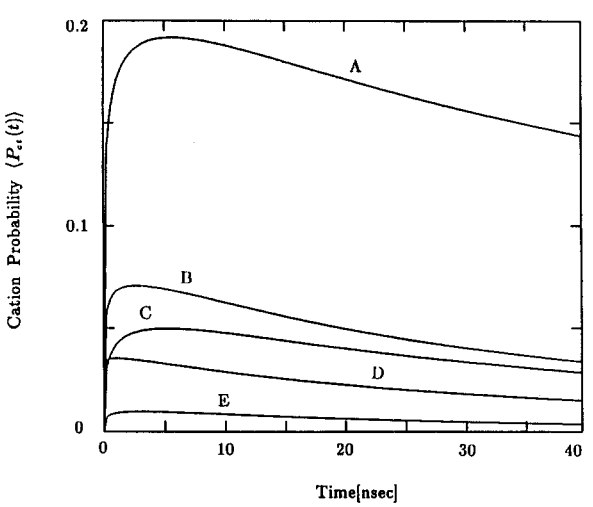

FIG. 3. The ensemble averaged cation probability for various parameters. Each curve shows an abrupt rise at short times and then a long decay. $C = 0.1$ M and $\tau = 16$ ns in all curves. (A) $a_f = a_b = 1.0$ Å, $R_0 = 13$ Å, $R_b = 10$ Å. (B) $a_f = a_b = 1.0$ Å, $R_0 = 13$ Å, $R_b = 13$ Å. (C) $a_f = a_b = 1.0$ Å, $R_0 = 10$ Å, $R_b = 10$ Å. (D) $a_f = a_b = 0.5$ Å, $R_0 = 13$ Å, $R_b = 13$ Å. (E) $a_f = a_b = 1.0$ Å, $R_0 = 10$ Å, $R_b = 13$ Å.

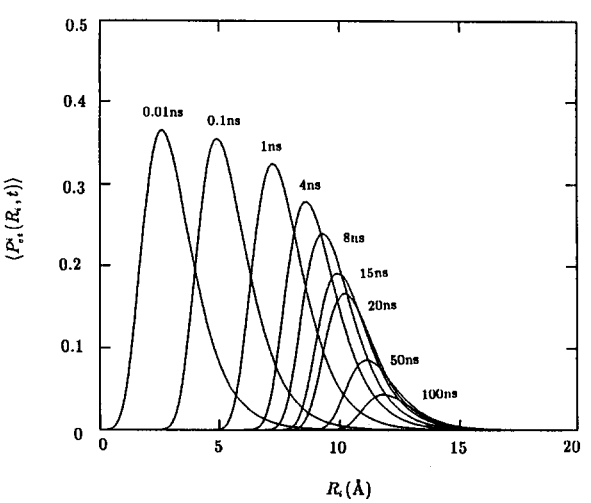

FIG. 4. The probability that the ith acceptor is an anion as a function of distance at particular times. At short times the anion lies close to the cation. At longer times the anion–cation separation moves out. $C = 0.1$ M, $\tau = 16$ ns, $R_0 = R_b = 10$ Å, and $a_f = a_b = 1$ Å.

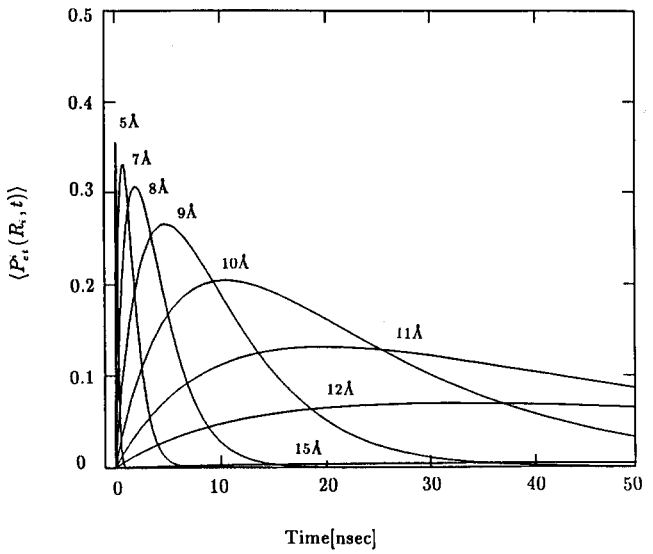

FIG. 5. The probability that the ith acceptor is an anion as a function of time at particular distances. This illustrates that short distance forward transfer and recombination occurs rapidly and long distance events are slower. $C = 0.1$ M, $\tau = 16$ ns, $R_0 = R_b = 10$ Å, and $a_f = a_b = 1$ Å.

At short times, most ion pairs that are created have very small ion separations. These pairs are created quickly, but because of the small separations, recombination is very rapid. Thus the pairs created at short time with small ion separations do not survive for very long. As time increases, the distribution of ion separation distances becomes larger. As can be seen from the figure, it is as if the distribution of separations moves out as a wave. Pairs with small separations are created and vanish. Then pairs with larger separations are created and vanish. It can also be seen from the figure that for a given set of parameters, there is an effective maximum separation. This arises because of the excited state lifetime which acts to cut off very slow, long range transfer events.

Figure 5 exhibits the dependence of $\langle P_{ct}^i(R_i,t)\rangle$ on the time for distances R_i varying from 5 to 15 Å. The parameters used in the calculation are the same as those in Fig. 4 and for curve C of Fig. 3. The curves in Fig. 5 are analogous to those in Fig. 4. For a given t, if the value for a particular distance is multiplied by $4\pi C R_i^2$ and then integration over all distance is carried out, the resulting number is the value of curve C in Fig. 3 at time t. Like Fig. 4, these curves give a feel for the partitioning of ion pair separations by time intervals. For example, at 5 ns, pairs separated by 5.0 Å have been created and recombined. Pairs with 7.0 Å separations have almost disappeared. There are still a significant number of pairs with 8.0 Å separations, but they are rapidly vanishing, while the probability of finding pairs with 9.0 Å separation is just reaching a maximum. The widths of the curves increase with increasing separation distance. The larger the separation between the cation and anion, the longer the radical pair survives.

C. Ion separations and existence times

In this section, the average separation between ions which make up a pair, $\langle R(t)\rangle$, and the average cation existence time $\langle \tau(R)\rangle$, are calculated. For pairs of ions, the average ion separation $\langle R(t)\rangle$ is defined as

$$\langle R(t)\rangle = \frac{4\pi\int_0^\infty \langle P_{ct}^i(R_i,t)\rangle R_i^3\, dR_i}{4\pi\int_0^\infty \langle P_{ct}^i(R_i,t)\rangle R_i^2\, dR_i}, \tag{16}$$

where $\langle P_{ct}^i(R_i,t)\rangle$ [Eq. (15)] is the ensemble averaged probability of finding an ion pair at time t with separation R_i. The integral in the denominator is a normalization factor.

Figure 6 plots the average ion separation as a function of time for various sets of electron transfer parameters. The concentration is 0.1 M, and the donor lifetime is 16 ns. The other parameters are also the same as those used in Fig. 3. For these sets of parameters an abrupt change is observed in the first nanosecond of each curve. The curves then become relatively flat. Consider curve C, this uses the same parameters as curve C of Fig. 3. Figure 3 displays the probability that a cation (ion pair) exists. The rapid increase in ion separation corresponds to the rapid increase in the cation probability. The ion pairs created at short time have small separations and recombine rapidly. The pairs which are created at longer time have larger separations and survive for much longer, giving rise to an increase in the average separation.

Comparing curves A and C, and curves B and E, it is seen that increasing R_0 increases the average ion separation, i.e., increasing the range of the forward transfer increases the average separation. While this is not surprising, it is less obvious that increasing R_b also increases the average separation. This can be seen by comparing curves A and B, and curves C and E. The increase in average separation is at the expense of total ion population as can be seen from the population curves in Fig. 3 for the same parameters. Figure 6 also shows the effect of changing a_f and a_b. Comparing curves B and D, it is seen that decreasing a_f and a_b causes the average separation to be relatively larger at short time but relatively smaller at long time. Equations (1b) and (1c) show that

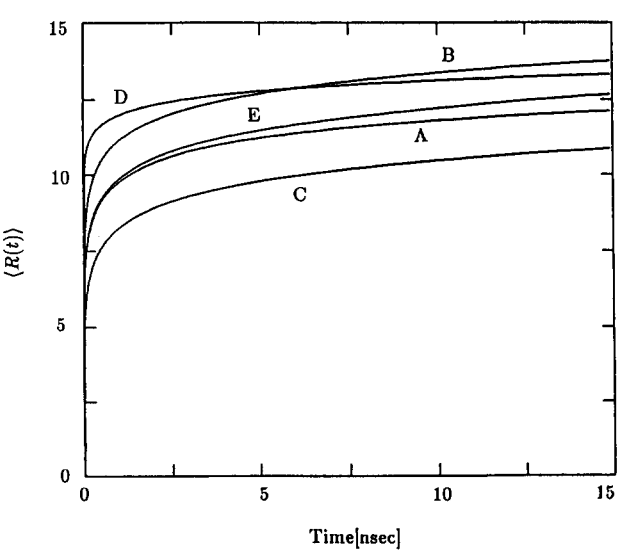

FIG. 6. The average ion separation as a function of time. The ion pairs with small separations recombine rapidly and are removed from the average over distance. The result is the fast increase in separation at short times. The parameters are the same as those used in Fig. 3.

reducing either a_f or a_b is equivalent to rescaling $R_0 - R$ or $R_b - R$, respectively. The result is to make the transfer rate faster for $R \leqslant R_0 (R \leqslant R_b)$ and slower for $R > R_0 (R > R_b)$. Therefore reducing a_f and a_b increases the short time average separation but decreases the long time separation.

The average cation existence time is defined as

$$\langle \tau(R_i) \rangle = \frac{\int_0^\infty t \langle P_{ct}^i (R_i,t) \rangle dt}{\int_0^\infty \langle P_{ct}^i (R_i,t) \rangle dt}, \tag{17}$$

where $t = 0$ is the time at which the ensemble of donors is excited. It is important to note that $\langle \tau(R_i) \rangle$ is not the average lifetime of the ion pairs, since the ion pairs are created at various times. Therefore, for a given ion separation the average existence time is a function of when the pairs are created and when back electron transfer returns the molecules to their neutral ground states. $\langle \tau(R_i) \rangle$ reflects the time at which ion pairs, with a particular ion separation, are likely to exist.

Figure 7 displays $\langle \tau(R_i) \rangle$ for various sets of electron transfer parameters. The parameters are the same as those used in Fig. 3. Consider curve C in Fig. 7. This corresponds to the cation probability curve C of Fig. 3. At 10 Å, the average existence time is 25 ns. At this time the cation probability is still substantial but tailing off. At 11.5 Å the existence time has increased to 100 ns. Figure 7 shows that the smallest distance scale one can probe in the electron transfer experiment is limited by the time resolution of the instrumentation. Again, considering curve C, with an experiment having 10 ns time resolution, the dynamics of ion pairs having separations of 9 Å or greater are probed. If the time resolution is reduced to 1 ns, distances on the order of 7 Å and greater are probed. It is clear that for the parameters of curve C, picosecond time resolution will be required to examine the creation and recombination of pairs with very small ion separations.

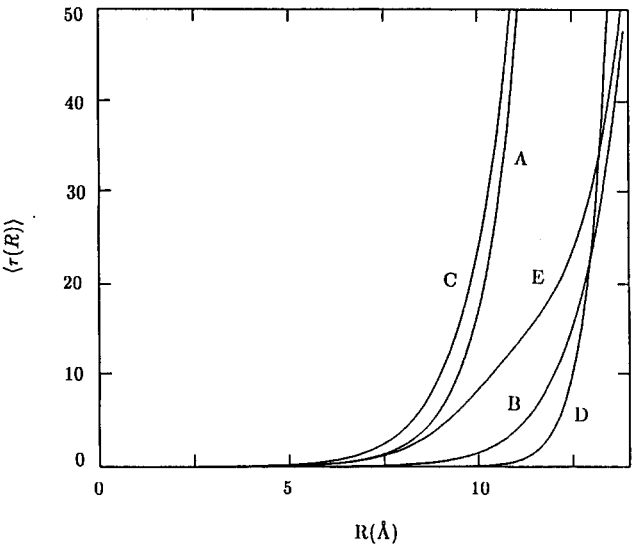

FIG. 7. The average ion existence time as a function of distance. At short distances ions will recombine rapidly while at larger distances ions will have longer existence times. The parameters are the same as those used in Fig. 3.

D. Excluded volume effects

In the theory presented in Sec. II and used to perform the calculations presented above, the donor and acceptor molecules were taken to be point particles in an infinite continuum. However, in real systems, molecules occupy finite volumes. Therefore, some of the spatial configurations which arise in the ensemble averages for point particles should be excluded. Two acceptor molecules, or acceptor and donor molecules, cannot have overlapping occupied volumes. At low concentrations, the number of configurations which are over counted is negligible and no correction for excluded volume is necessary to give an accurate result.

In the Appendix, the problem of electron transfer and back transfer is again considered, and excluded volume is incorporated in detail into the calculation. The full derivation is given in the Appendix. The final result is

$$\langle P_{ct}(t) \rangle = 4\pi C \int_{R_m}^\infty K_f(R_i) e^{-K_b(R_i)t} \int_0^t \exp\{-[K_f(R_i) - K_b(R_i)]t'\}$$
$$\times e^{-t'/\tau} \exp\left(-4\pi d^{-3} \sum_{k=1}^\infty \frac{p^k}{k} \int_{R_m}^\infty (1 - e^{-t' K_f(R_j)})^k R_j^2 \, dR_j \right) dt' \, R_i^2 dR_i, \tag{18}$$

where d is the diameter of the acceptor excluded volume and p is Cd^3. R_m is the sum of the radii of donor and acceptor excluded volumes. The first term in k of this result is Eq. (14). In the limit of low concentration or small acceptor size the higher order terms become insignificant and Eq. (18) reduces to Eq. (14), the point particle result. At high concentrations terms are calculated in Eq. (18) until convergence is reached.

Figures 8 and 9 display calculations of cation probabilities as a function of time as in Fig. 3. The concentrations of the acceptors vary from 0.1 to 1.0 M, and other electron transfer parameters are listed in the figure captions. In these calculations the molecules occupy volumes which corresponds to spheres of diameter 6 Å. This volume is comparable to a common acceptor molecule, benzoquinone. For each concentration, three curves are plotted, one without excluded volume (CN), which is given by Eq. (14), one with only donor–acceptor excluded volume (CC), and one with

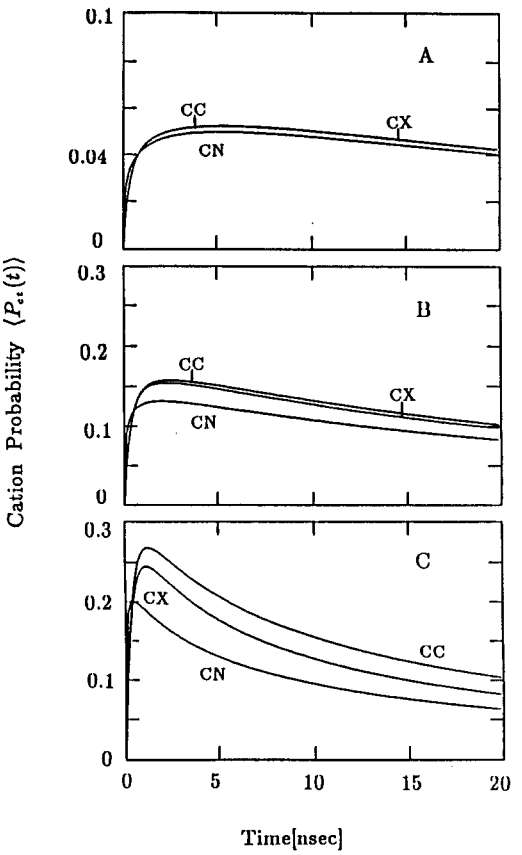

FIG. 8. The cation probability with excluded volume effects. Three types of curves are plotted. The curves labeled CN do not include excluded volume effects. The curves labeled CC include donor–acceptor excluded volume only. The curves labeled CX are the full excluded volume calculations, i.e., they have donor–acceptor and acceptor–acceptor effects included. The parameters are: $R_0 = R_b = 10$ Å, $a_f = a_b = 1$ Å, $\tau = 16$ ns and the concentrations are $C = 0.1$, 0.4, and 1.0 M.

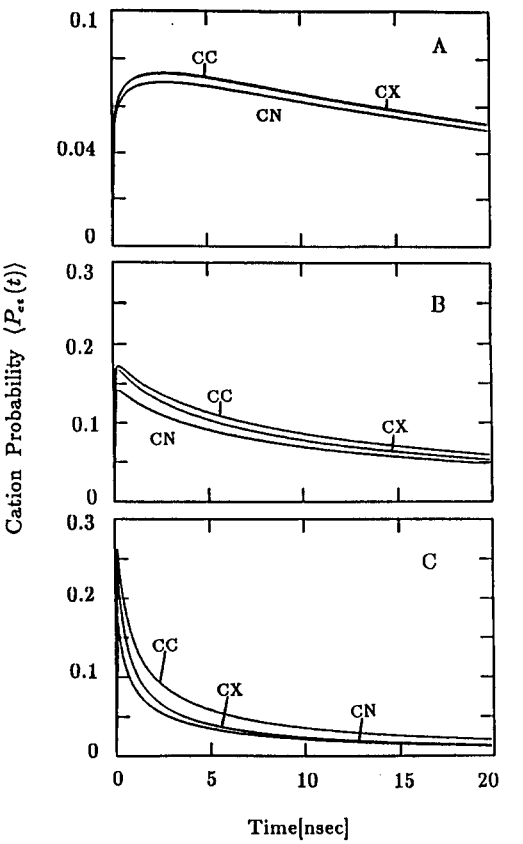

FIG. 9. The cation probability with excluded volume effects for a different set of parameters. CN, CC, and CX have the same meaning as in Fig. 8. The parameters are: $R_0 = R_b = 13$ Å, $a_f = a_b = 1.0$ Å, $\tau = 16$ ns and the concentrations are $C = 0.1$, 0.4, and 1.0 M.

both donor–acceptor and acceptor–acceptor excluded volume (CX), which is given by Eq. (18). The inclusion of only donor–acceptor excluded volume in the calculation of the cation probability is obtained by using a cutoff R_m in the lower limit of the integration in Eq. (14).

The concentration at which excluded volume can no longer be ignored depends not only on the excluded volumes but also on the system's electron transfer parameters. R_m, which accounts for donor–acceptor excluded volume, is effectively a rate cutoff. R_0 and R_b, which have been defined in Sec. II, are the distances at which the forward and back transfer rates respectively, are equal to the rate of fluorescence, $1/\tau$. At distances shorter than R_0 and R_b the rates of forward and back transfer are faster than $1/\tau$. At longer distances the transfer rates are slower than $1/\tau$. If R_m is very small compared to R_0 and R_b then the effect of donor–acceptor excluded volume is negligible. If R_m is some significant fraction of R_0 and R_b, and if the concentration is sufficiently high to give a reasonable probability of finding an acceptor in a volume with radius R_m, then the averages will be different from the point particle case. The cutoff will exclude many of the fast transfer contributors from the averages.

The acceptor–acceptor excluded volume cannot be included by a simple cutoff (see the Appendix). The correction for acceptor–acceptor excluded volume eliminates the configurations from the calculations in which two acceptors have overlapping volumes. These are included in the point particle calculations.

As concentration becomes high, in Figs. 8 and 9, the curves CC, CX, and CN become increasingly different. At concentrations less than 0.1 M the effect of excluded volume is negligible for the given parameters and the three types of curves are essentially the same. For increasingly high concentrations, the differences between CC, CX, and CN grow. The $C = 0.1$ M curves in both Figs. 8 and 9 show that the first change arises from donor–acceptor excluded volume. The CC and CX curves are indistinguishable and somewhat above the CN curves. The $C = 0.4$ M curves display larger differences. The CC and CX calculations are no longer the same. The full excluded volume calculation CX curves, are above the CN curves but below the CC curves. This is also true of the $C = 1.0$ M curves, and is true in general. Including only donor–acceptor excluded volume (CC) over estimates the excluded volume effect. The acceptor–acceptor excluded volume acts in opposition to the donor–acceptor excluded volume.

The calculations presented in the previous sections used an acceptor concentration of 0.1 M. Figures 8 and 9 show that at this concentration the difference between the point particle model and full excluded volume calculation is small. When analyzing experimental data, the results of Sec. II and

the Appendix can be used to determine the magnitude of excluded volume effects.

IV. EXPERIMENTAL OBSERVABLES

The dynamics of electron transfer and back transfer are determined by five molecular parameters and the concentration of the acceptors in the sample. In addition to the donor excited state lifetime, there are four parameters, a_f and R_0 (forward transfer parameters), and a_b and R_b (backward transfer parameters). The forward transfer parameters can be determined by a combination of concentration dependent steady state fluorescence quenching and time resolved fluorescence quenching experiments.[20,22] With knowledge of these parameters, the backward parameters can be obtained from a ground state recovery experiment. The most common ground state recovery method is a probe pulse experiment. Probe pulse experiments, however, generally have problems with dynamic range because it is necessary to measure a small change in a large signal. Here we will discuss another technique, a transient grating experiment. This is a zero background technique which helps avoid a variety of artifacts which can occur in a probe pulse experiment.[24] The two types of experiments are closely related, and an expression for the probe pulse experiment is given below.

In a transient grating experiment, two excitation pulses, tuned to the donor absorption wavelength, are crossed at a small angle in the sample. The optical interference between the two coherently related pulses generates alternating regions of light and dark, i.e., an interference pattern. In the peaks of the pattern (light regions) absorption by donors occurs. In the nulls (dark regions) no absorption takes place. Electron transfer will occur in the peaks of the pattern. The peaks which have excited states and ion pairs have a different index of refraction than the nulls where there are only ground state molecules. Thus there is a spatially periodic variation in the samples complex index of refraction. This acts as a Bragg diffraction grating for a variably delayed probe pulse brought into the sample at an angle to meet the Bragg condition for the grating. A fourth beam of light, the part of the probe pulse diffracted from the grating, is the signal. It leaves the sample in a unique direction determined by the Bragg condition. This provides the zero background signal. As the excited states decay and the ion pairs recombine, the grating decays. As the grating decays, the intensity of the diffracted signal decreases. Thus, monitoring the decay of the diffracted light as a function of the delay of the probe pulse measures the decay of excited states and the recombination of ion pairs.

The transient grating signal $S(t)$ is proportional to the square of the peak–null difference in the complex index of refraction of the medium.[25] For the treatment outlined here, it is assumed that the probe pulse is tuned to the peak of the donor absorption and that this wavelength is not absorbed by donor excited states or by the ions. Thus the grating is due to ground state depletion. Other possible contributions to the signal, e.g., excited state gratings, ion absorption gratings, or triplet gratings (arising from intersystem crossing) can be added when warranted by experimental conditions.

$S(t)$ is given by

$$S(t) = A(\tilde{n}_p - \tilde{n}_n)^2, \tag{19}$$

where $\tilde{n}_p$ and $\tilde{n}_n$ are the complex indices of refraction at grating peaks and nulls, respectively, and

$$\tilde{n}_{p,n} = n_{p,n} + ik_{p,n}. \tag{20}$$

Combining Eqs. (19) and (20) gives

$$S(t) = B_1(n_p - n_n)^2 + B_2(k_p - k_n)^2. \tag{21}$$

The first term in Eq. (21) accounts for the phase grating (real part of the index) diffraction, and the second term accounts for the amplitude grating (imaginary part of the index) diffraction. For a probe wavelength tuned to the peak of the donor absorption, the contribution from the phase grating becomes negligible. Thus,

$$S(t) = B_2(k_p - k_n)^2, \tag{22}$$

k_p and k_n are the imaginary contributions to the index of refraction at grating peaks and nulls, respectively.

The k's are related to the optical densities D at the probe wavelength by

$$D = \frac{4\pi lk}{2.3\lambda}, \tag{23}$$

where l is the sample thickness and λ is the probe wavelength. Collecting constants,

$$S(t) = Q(D_p - D_n)^2. \tag{24}$$

Thus the signal is proportional to the peak–null difference in the optical density. Since $D = \epsilon lC$, where ϵ is the donor extinction coefficient at the probe wavelength and C is the concentration,

$$S(t) = Q\epsilon^2 l^2 (C_p - C_n)^2. \tag{25}$$

C_n is the concentration of ground state neutral donor molecules in the grating nulls. Since there are no excited states or ion pairs produced in the nulls, C_n is the concentration of donors in the sample, C. C_p is the concentration of ground state neutral donors in the grating peaks. It is less than C because of the existence of donor excited states and ion pairs.

$$C_p = C\,[1 - \langle P_{ex}(t)\rangle - \langle P_{ct}(t)\rangle]. \tag{26}$$

Substituting, the transient grating signal is

$$S(t) = Q\epsilon^2 l^2 C^2 [\langle P_{ex}(t)\rangle + \langle P_{ct}(t)\rangle]^2. \tag{27}$$

Equation (27) shows that the transient grating signal is proportional to the square of number of donor molecules not in their neutral ground state, i.e., the number of donors which are electronically excited or which are cations. The time dependence of the transient grating signal is the square of the time dependent signal in a probe pulse experiment. If the probe wavelength is not tuned to the maximum of the donor absorption, there will also be a phase grating contribution. This is proportional to the amplitude grating contribution, so the time dependent signal given in Eq. (27) is independent of the probe wavelength as long as the only probe absorption is due to ground state neutral donor molecules. If there are excited state or ionic absorptions, terms are added to account for the additional amplitude and phase grating diffraction. It is straightforward to test for other absorptions

by tuning the probe wavelength within the donor absorption peak. If the time dependence is independent of probe wavelength, only donor absorption is contributing to the signal.

Equation (27) displays the direct connection between the transient grating signal and the electron transfer parameters. Since the forward electron transfer parameters, which come into the determination of $\langle P_{ex}(t)\rangle$, can be independently measured with fluorescence quenching experiments, the two unknown parameters, the electron back transfer parameters a_b and R_b which enter into $\langle P_{ct}(t)\rangle$, can be determined from the grating measurements. Initial experiments of this kind have been reported recently.[22] A detailed comparison between the theory presented in Sec. II and the Appendix and experiment will be given in a subsequent publication.[23]

ACKNOWLEDGMENT

This work was supported by the Department of Energy, Office of Basic Energy Sciences (DE-FG03-84ER13251).

APPENDIX: $\langle P_{ct}(t)\rangle$ WITH EXCLUDED VOLUME

The theory developed in Sec. II used a model of point particles distributed randomly in a solid solution. In a real molecular system, the donor and acceptor molecules occupy finite volumes. In performing the averages over all spatial configurations which led to Eq. (14), configurations were included which are not possible for particles with finite volumes. In this appendix, the problem of electron transfer and back transfer is reconsidered taking into account excluded volume. The final result is Eq. (A13) also given in Sec. III D as Eq. (18).

The ensemble average over a continuum with consideration of donor–acceptor and acceptor–acceptor excluded volume is a mathematically formidable task. In order to avoid complicated multidimensional integrals which take into account acceptor–acceptor excluded volume, we first attack the problem using a discrete lattice model. We will derive, without acceptor–acceptor excluded volume, the cation probability $\langle P_{ct}(t)\rangle$ on a lattice. The inclusion of the donor–acceptor and acceptor–acceptor excluded volume effects in a lattice calculation of forward transfer $[\langle P_{ex}(t)\rangle]$ has been derived by others.[26–28] We will use it to calculate the cation probability that includes excluded volume effects. The comparison betwen these two lattice models allows us to isolate the contribution of excluded volume. Finally by going to the continuum limit we obtain a quantitative description of the cation probability with excluded volume.

The derivation of the cation probability in the lattice model, without acceptor–acceptor excluded volume, begins with Eq. (9):

$$\langle P^i_{ct}(R_i,t)\rangle_{n-1,N} = \int_0^t K_f(R_i)\exp[-K_b(R_i)(t-t')] \times \langle P_{ex}(R_i,t')\rangle_{n-1,N}dt'. \tag{A1}$$

This is the probability that the ith acceptor is an anion in the presence of $n-1$ other acceptors occupying N lattice sites. The average over the $n-1$ acceptors reduces the problem to one acceptor in the presence of the averaged effect of the other acceptors. In the one acceptor case, acceptor–acceptor excluded volume does not play a role because the single acceptor can be located anywhere in space. Thus, the average over the ith acceptor may be done as in the continuum:

$$\langle P_{ct}(t)\rangle_{n,N} = \frac{4\pi n}{V}\int_{R_m}^{R_v}\langle P^i_{ct}(R_i,t)\rangle_{n-1,N}R_i^2\,dR_i. \tag{A2}$$

In the prefactor, V is the volume. R_m accounts for the finite size of the donor and acceptor.

Substituting Eq. (A1) into Eq. (A2) gives

$$\langle P_{ct}(t)\rangle_{n,N} = \frac{4\pi n}{V}\int_{R_m}^{R_v}\int_0^t K_f(R_i)e^{-K_b(R_i)(t-t')} \times\langle P_{ex}(R_i,t')\rangle_{n-1,N}dt'\,R_i^2\,dR_i, \tag{A3}$$

where $R_v = [3V/(4\pi)]^{1/3}$. (A3)

To obtain the observable, it is necessary to pass to the thermodynamic limit:

$$\langle P_{ct}(t) = \lim_{n,N\to\infty}\langle P_{ct}(t)\rangle_{n,N} \tag{A4}$$

Substituting Eq. (A3) into Eq. (A4) gives

$$\langle P_{ct}(t)\rangle = 4\pi C\int_{R_m}^{\infty}\int_0^t K_f(R_i)e^{-K_b(R_i)(t-t')} \times\left[\lim_{n,N\to\infty}\langle P_{ex}(R_i,t')\rangle_{n-1,N}\right]dt'\,R_i^2\,dR_i. \tag{A5}$$

The factor inside the brackets has been evaluated for a continuum without donor excluded volume in Sec. II. For a cubic lattice the derivation begins with Eq. (4):

$$P_{ex}(t) = e^{-kt}\exp\left[-\sum_{i=1}^{n}K_f(R_i)t\right]. \tag{4}$$

Performing the average over $n-1$ acceptors on N lattice sites gives

$$\langle P_{ex}(R_i,t)\rangle_{n-1,N} = e^{-kt}e^{-K_f(R_i)t}\left(\frac{1}{N}\sum_{j=1}^{N}e^{-K_f(R_j)t}\right)^{n-1}. \tag{A6}$$

Here the sum is over the N lattice sites rather than an integral over the volume. Taking the thermodynamic limit gives

$$\begin{aligned}\langle P_{ex}(R_i,t)\rangle &= e^{-kt}e^{-K_f(R_i)t}\lim_{n,N\to\infty}\left(\frac{1}{N}\sum_{j=1}^{N}e^{-K_f(R_j)t}\right)^{n-1}\\ &= e^{-kt}e^{-K_f(R_i)t}\exp\left[-Cd^3\sum_{j=1}^{\infty}(1-e^{-K_f(R_j)t})\right],\end{aligned} \tag{A7}$$

where $V = Nd^3$ and d is the lattice constant. This equation does not take into account acceptor–acceptor excluded volume. Here any number of acceptors may occupy a single lattice site. Acceptors are not allowed to occupy the origin (the donor site) maintaining an excluded volume around the donor equal to d^3. Substituting Eq. (A7) into Eq. (A5) gives the cation probability for donors on a cubic lattice with acceptors:

$$\langle P_{ct}(t)\rangle = 4\pi C \int_{R_m}^{\infty}\int_0^t K_f(R_i) e^{-K_b(R_i)(t-t')} e^{-K_f(R_i)t'} \exp\left[-kt' - Cd^3 \sum_{j=1}^{\infty}(1-e^{-K_f(R_j)t'})\right] R_i^2\, dR_i\, dt'. \tag{A8}$$

The lattice sum in Eq. (A8) for a cubic lattice is given explicitly by

$$\begin{aligned}\sum_{j=1}^{\infty}\{1-\exp[-K_f(R_j)]t\} = \sum_{j=1}^{\infty}\Big(&6\{1-\exp[-K_f(jd)t]\} + 8\{1-\exp[-K_f(\sqrt{3}jd)t]\} \\ &+ 12\sum_{k=1}^{j}\{1-\exp[-K_f(\sqrt{j^2+k^2}d)t]\}(2-\delta_{kj}) \\ &+ 24\sum_{l=1}^{j}\sum_{k=1}^{j-1}\{1-\exp[-K_f(\sqrt{j^2+l^2+k^2}d)t]\}\Big).\end{aligned} \tag{A9}$$

The inclusion of acceptor–acceptor excluded volume in the derivation of the factor in brackets in Eq. (A5) has been derived by others.[26,27] The result is

$$\begin{aligned}\langle P_{ex}(R_i,t)\rangle &= \exp\{-[k+K_f(R_i)]t\}\prod_{j=1}^{\infty}[1-p+pe^{-K_f(R_j)t}] \\ &= \exp\{-[k+K_f(R_i)]t\}\prod_{j=1}^{\infty}[1-Cd^3+Cd^3e^{-K_f(R_j)t}],\end{aligned} \tag{A10}$$

where the product is over the lattice sites. Substituting this result into Eq. (A5) gives the cation probability for acceptors on a cubic lattice with acceptor–acceptor excluded volume:

$$\langle P_{ct}(t)\rangle = 4\pi C \int_{R_m}^{\infty}\int_0^t K_f(R_i) e^{-K_b(R_i)(t-t')} e^{-K_f(R_i)t'} e^{-kt'} \prod_{j=1}^{\infty}[1-p+pe^{-K_f(R_j)t'}] R_i^2\, dR_i\, dt'. \tag{A11}$$

The system we are interested in is a continuum. It is possible to extend Eq. (A10) to a continuum[27,28] by changing the product in Eq. (A10) to an exponential of a lattice sum, then taking the logarithm, and replacing the sum by an integral. The result is

$$\langle P_{ex}(R_i,t)\rangle = \exp\{-[k+K_f(R_i)]t\}\exp\left(-4\pi d^{-3}\sum_{k=1}^{\infty}\frac{p^k}{k}\int_{R_m}^{\infty}(1-e^{-tK_f(R_j)})^k R_j^2\, dR_j\right). \tag{A12}$$

Substituting this into Eq. (A5) gives the cation probability for a continuum with donor–acceptor and acceptor–acceptor excluded volume:

$$\begin{aligned}\langle P_{ct}(t)\rangle = 4\pi C \int_{R_m}^{\infty}\int_0^t &K_f(R_i) e^{-K_b(R_i)(t-t')} e^{-K_f(R_i)t'} \\ &\times e^{-t'/\tau}\exp\left[-4\pi d^{-3}\sum_{k=1}^{\infty}\frac{p^k}{k}\int_{R_m}^{\infty}(1-e^{-t'K_f(R_j)})^k R_j^2\, dR_j\right] R_i^2\, dR_i\, dt',\end{aligned} \tag{A13}$$

where R_m is the sum of the radii of the donor and acceptor volumes, and d is the diameter of the acceptor volume. Equation (A13) is discussed in Sec. III D.

[1] T. Guarr and G. McLendon, Coord. Chem. Rev. **68**, 1 (1985).
[2] D. Devault, Q. Rev. Biophys. **13**, 387 (1980).
[3] Z. D. Popovic, G. J. Kovacs, and P. S. Vincett, Chem. Phys. Lett. **116**, 405 (1985).
[4] S. F. Fischer and P. O. Scherer, Chem. Phys. **115**, 151 (1987).
[5] Y. Nosaka, H. Miyama, M. Terauchi, and T. Kobayashi, J. Phys. Chem. **92**, 255 (1988).
[6] T. Kakitani and N. Mataga, J. Phys. Chem. **89**, 8 (1985).
[7] H. Miyasaka and N. Mataga, Chem. Phys. Lett. **134**, 480 (1987).
[8] C. L. Braun and T. W. Scott, J. Phys. Chem. **91**, 4436 (1987).
[9] Z. Schulten and K. Schulten, J. Chem. Phys. **66**, 4616 (1977).
[10] H. J. Werner, Z. Schulten, and K. Schulten, J. Chem. Phys. **67**, 646 (1977).
[11] R. C. Dorfman, Y. Lin, and M. D. Fayer, J. Chem. Phys. (to be published).
[12] P. Siders and R. A. Marcus, J. Am. Chem. Soc. **103**, 748 (1981).
[13] J. N. Onuchic, D. N. Beratan, and J. J. Hopfield, J. Phys. Chem. **90**, 3707 (1986).
[14] N. Sutin, Acc. Chem. Res. **15**, 275 (1982).
[15] N. R. Kestner, J. Logan, and J. Jortner, J. Phys. Chem. **78**, 2148 (1974).

[16]R. K. Huddleston and J. R. Miller, J. Phys. Chem. **86**, 200 (1982).
[17]R. P. Domingue and M. D. Fayer, J. Chem. Phys. **83**, 2242 (1985).
[18]P. Siders, R. J. Cave, and R. A. Marcus, J. Chem. Phys. **81**, 5613 (1984).
[19]S. Strauch, G. Mclendon, M. McGuire, and T. Guarr, J. Phys. Chem. **87**, 3579 (1983).
[20]M. Inokuti and F. Hirayama, J. Chem. Phys. **43**, 1978 (1965).
[21]J. R. Miller, J. V. Beitz, and R. K. Huddleston, J. Am. Chem. Soc. **106**, 5057 (1984).
[22]R. C. Dorfman, Y. Lin, and M. D. Fayer, J. Phys. Chem. **92**, 4258 (1988).
[23]R. C. Dorfman, Y. Lin, and M. D. Fayer, J. Phys. Chem. (to be published).
[24]M. D. Fayer, Annu. Rev. Phys. Chem. **33**, 63 (1982).
[25]K. Nelson, R. Casalegno, R. J. Dwayne Miller, and M. D. Fayer, J. Chem. Phys. **77**, 1144 (1982).
[26]A. Blumen and J. Manz, J. Chem. Phys. **71**, 4694 (1979).
[27]A. Blumen, J. Chem. Phys. **72**, 1632 (1980).
[28]J. Baumann and M. D. Fayer, J. Chem. Phys. **85**, 4087 (1986).